

Article

Irradiation Temperature Dependence of Shape Elongation of Metal Nanoparticles in Silica: Counterevidence to Ion Hammering Related Scenario

Hiroshi Amekura ^{1,*} , Saif Ahmad Khan ², Pawan Kumar Kulriya ^{2,3}  and Debdulal Kabiraj ²

¹ National Institute for Materials Science (NIMS), Tsukuba 305-0003, Ibaraki, Japan

² Inter-University Accelerator Centre (IUAC), Aruna Asaf Ali Marg, New Delhi 110067, India; khansaifahmad@gmail.com (S.A.K.); pkkulriya@mail.jnu.ac.in (P.K.K.); d.kabiraj@gmail.com (D.K.)

³ School of Physical Sciences, Jawaharlal Nehru University, New Mehrauli Road, New Delhi 110067, India

* Correspondence: amekura.hiroshi@nims.go.jp; Tel.: +81-29-863-5479

Abstract: Irradiation temperature (IT) dependence of the elongation efficiency of vanadium nanoparticles (NPs) in SiO₂ was evaluated: The samples were irradiated with 120 MeV Ag⁹⁺ ions to a fluence of 1.0×10^{14} ions/cm² each at ITs of 300, 433, 515, and 591 K, while the measurements were performed at room temperature. The vanadium was selected for the NP species because of the highest bulk m.p. of 1910 °C (2183 K) among all the species of the elemental metal NPs in which the shape elongation was observed. The highest m.p. could contribute negligible size changes of NPs against inevitable exposure to high temperatures for the IT dependence measurements. The elongation of V NPs was evaluated qualitatively by transmission electron microscopy (TEM) and quantitatively by optical linear dichroism (OLD) spectroscopy. The electron microscopy studies showed a pronounced elongation of NPs with ion irradiation at the elevated temperatures. The OLD signal was almost constant, or even slightly increased with increasing the IT from 300 to 591 K. This IT dependence provides a striking contrast to that of the ion hammering (IH) effect, which predicts a steep decrease with increasing IT. Combined with the other two counterevidence previously reported, the IH-related effect is excluded from the origin of the shape elongation of metal NPs in SiO₂.

Keywords: shape elongation; metal nanoparticle; swift heavy ion; irradiation temperature dependence; ion shaping; optical linear dichroism spectroscopy; silica glass



Citation: Amekura, H.; Khan, S.A.; Kulriya, P.K.; Kabiraj, D. Irradiation Temperature Dependence of Shape Elongation of Metal Nanoparticles in Silica: Counterevidence to Ion Hammering Related Scenario. *Quantum Beam Sci.* **2023**, *7*, 12. <https://doi.org/10.3390/qubs7020012>

Academic Editors: Hiroyuki Aoki, Alessandro Genoni and Masaki Oura

Received: 21 February 2023

Revised: 20 March 2023

Accepted: 24 March 2023

Published: 7 April 2023



Copyright: © 2023 by the authors. Licensee MDPI, Basel, Switzerland. This article is an open access article distributed under the terms and conditions of the Creative Commons Attribution (CC BY) license (<https://creativecommons.org/licenses/by/4.0/>).

1. Introduction

1.1. Shape Elongation of Metal Nanoparticles and the Ion Hammering Mechanism

In 2003, D’Orleans et al. discovered the shape transformation of metal nanoparticles (NPs) embedded in silica glass (SiO₂), from nearly spherical shapes to prolate spheroids or nano-rods, which was induced under swift heavy ion (SHI) irradiation [1]. The researchers prepared nearly spherical Co NPs of a mean diameter of ~10 nm by implanting 160 keV Co ions into SiO₂ layers on Si at an elevated temperature of 873 K [1]. Then they irradiated the spherical Co NPs embedded in SiO₂ with swift heavy ions of 200 MeV iodine ions. By increasing the fluence to 10¹³ ions/cm², some spherical NPs transformed into lemon shapes. Further increasing to 10¹⁴ ions/cm², they transformed into nano-rods [1]; i.e., NPs expand parallel to the ion beam and shrink perpendicular to it. An important property of this phenomenon was that the major axes of the elongated NPs were parallel with each other, which were also parallel to the SHI beam.

One year later, i.e., in 2004, a similar phenomenon was observed in a different configuration: The elongation was induced in the Au-cores of free-standing Au-core/silica-shell colloidal NPs under SHI irradiation [2], which were synthesized by a wet-chemical method. The spherical gold cores of 14 nm in diameter elongated along the SHI beam direction and transformed to rods of 6 nm in diameter and 54 nm in length under 30 MeV selenium (Se)

ion irradiation to a fluence of 2×10^{14} ions/cm². At the same time, the silica shells exhibited a completely different shape-transformation to oblate spheroids, i.e., shrinkage parallel to and expansion perpendicular to the SHI beam [2]. Since pure silica NPs were known to exhibit the same shape transformation to the oblate spheroids by the ion hammering (IH) effect [3], the shape transformation of the silica shells to the oblate spheroids was also ascribed to the IH effect [2]. To clarify the relationship between silica shells and the elongation of the Au-cores, core/shell NPs with different shell thicknesses ranging from 15 to 72 nm, but fixing the core diameter to 14 nm were synthesized and irradiated with 30 MeV Se ions. The elongation in the Au cores was observed with the particles having silica shells thicker than 26 nm only. The Au cores with thinner silica shells did not show an elongation. From these observations, it was considered that the silica shells were essential to induce the elongation of Au cores. The elongation of the Au-cores could be induced by the deformation of the silica shells, which could be induced by the IH effect [2]. The same mechanism was presumed for the elongation of the metal NPs embedded in films/bulk of silica.

However, it was pointed out that the IH effect was able to build up stress to the order of 100 MPa only, which is too low to induce the clearly observed deformation of solid Au NPs. Therefore, any radiation-induced softening of Au NPs was assumed. However, the observed large NP elongation cannot be ascribed to any known mechanisms of radiation-induced softening [4]. Then the synergy effect [5] was proposed between the in-plane stress accumulation by the IH effect and the transient melting, i.e., a kind of softening, of NPs by the inelastic thermal spike (i-TS) effect [6].

In this model, an isolated impact of SHI on the sample cannot induce the elongation of NP. Multiple impacts are necessary to induce the elongation: The first impact, and possibly some successive impacts, generate the in-plane stress in a certain region of the sample via the IH effect. When an ion finally hits an NP located within the previously generated in-plane stress, the NP becomes a molten phase by the i-TS effect and deforms following the in-plane stress. Because the elongation requires the multiple impacts of SHIs, the fluence dependence of the elongation of NPs should be non-linear with the fluence and could have a threshold along the fluence.

1.2. Counterevidence to the Ion Hammering Mechanism

Contrarily, Leino et al. have developed the two-temperature molecular dynamics (TT-MD) model, which is a combination of the classical molecular dynamics and the inelastic thermal spike model, and have reproduced the shape elongation of Au NP in SiO₂ [7]. The simulations show that an NP is elongated by only one impact of an SHI. The authors ascribed the elongation mechanism to “thermal pressure and flow”. The elongation of NPs is induced by the mass transfer of molten metal through the low-density cores in silica simultaneously generated by the i-TS effect [7].

To judge which mechanism is more probable, we have measured the fluence dependence of the NP elongation down to low fluences of $\sim 1 \times 10^{11}$ ions/cm², where track overlaps are negligible. Optical linear dichroism (OLD) spectroscopy [8] was applied since this is a sensitive method to detect the elongation of metal NPs even at low fluences. In this method, the optical absorption is detected under the illumination of linearly polarized light either parallel or perpendicular to the major axes of the NPs. Then the difference between the two polarizations (0 and 90°) is evaluated. The difference should be null for spherical NPs because there is no special direction in a sphere. However, once the elongation is induced, the difference signal is detected. In this method, a region of a few mm in diameter was illuminated. Since the signal is averaged over a macroscopic number of NPs included in the millimeter dimension, the sensitivity is quite high.

In fact, we have observed an elongation signal from irradiated Zn NPs in silica down to 1×10^{11} ions/cm², where the track overlaps are negligible [8]. This observation contradicts the synergy effect of the IH and the NP melting and rather supports that the elongation is induced by a single impact of SHI. Furthermore, silica shows radiation-induced compaction

(densification) at very low fluences where overlaps of tracks are negligible. When tracks are overlapped, the compaction transforms into the IH effect [9]. Consequently, the observed linear fluence dependence of the NP elongation without the threshold is totally inconsistent with the IH effect [10].

Another counterevidence to the IH effect is the relationship between the ion incident angles and the elongation angles of NPs [11]. Since the angular dependence of the deformation tensor A of the IH effect has off-diagonal components, the ion incident angle is not always expected to be the same as the elongation angle of the NPs due to the IH effect. While the IH effect suggested a complicated relationship between the ion incident angle and the elongation angle of NPs, the same angles were observed within experimental errors between the ion incident angles and the elongation angles of NPs [12].

While the above two observations have been proposed as counterevidence to the IH effect involved in the mechanism of the elongation of NPs, we propose in this paper the third counterevidence to the IH effect, i.e., the different irradiation temperature (IT) dependences between the elongation of NPs and the IH effect. While the deformation efficiency of the IH effect monotonically decreases with the IT from 300 to 650 K [9], the elongation efficiency of NPs was almost constant or rather slightly increases between 300 K and 591 K as described below.

2. Materials and Methods

To study the IT dependence of the elongation efficiency of metal NPs, the NPs of vanadium were selected, because of its highest bulk melting point (m.p.) of 1910 °C (2183 K) [13] among all the species of elemental metal NPs which have shown shape elongation. It is known that some changes induced in metals by increasing temperature T can be normalized by a ratio of T/T_m between different metals, where T_m denotes the melting temperature. Therefore, the highest melting temperature of V is advantageous to minimize the thermally induced size changes in NPs. In fact, we have compared the thermal stability of elongated Zn and V NPs in SiO₂ under isochronal annealing, both of which were irradiated with 200 MeV Xe ions to the same fluence [14] prior to the annealing. The elongated shapes of Zn NPs were maintained up to 400 °C (673 K) but were recovered to the spherical shapes exceeding 400 °C (673 K). Contrarily, V NPs maintained the elongated shapes up to a much higher temperature of 800 °C (1073 K) [14], which indicates much higher thermal stability of V NPs over Zn NPs.

Vanadium NPs in nearly spherical shapes were fabricated in silica glass of KU-1 type (OH concentration of ~820 ppm) by implanting 60 keV V⁺ ions to a fluence of 1.0×10^{17} ions/cm². V NPs were formed without post-implantation annealing. According to our past literature [15], the NPs with a mean diameter of 9.0 nm and a standard deviation of 2.9 nm were formed within the surface layer of ~70 nm in thickness.

The V NPs embedded in SiO₂ were irradiated with 120 MeV Ag⁹⁺ ions to a fluence of 1×10^{14} ions/cm² at constant temperatures of 300, 433, 515, and 591 K using a high-temperature irradiation chamber [16] in the Inter-University Accelerator Centre (IUAC), New Delhi, India. The samples were irradiated at an incident angle of 45° from the surface normal to evaluate the degree of the elongation by the optical linear dichroism (OLD) spectroscopy [8,14], in addition to transmission electron microscopy (TEM).

Since the high fluence of 1×10^{14} ions/cm² required a relatively long irradiation time of ~5 h, the NPs were maintained at a higher temperature than room temperature (RT) in the irradiation chamber in a vacuum for ~5 h during the irradiation. These high-temperature processes might change the NP sizes. This point is important because the initial sizes of the NPs affect the elongation efficiency [17]. Therefore, three or four sets of samples were prepared for each IT. See Table 1: One set of the samples was annealed in a vacuum at 591 K, i.e., the highest IT, for 5 h before the irradiations at each IT, to maximize the thermally induced coarsening of NPs, if induced. The 2nd set of samples was irradiated at each IT without pre-irradiation annealing. The 3rd set was mounted in the high-temperature irradiation chamber and maintained at the IT for 5 h but not irradiated.

From the comparisons of the two groups (with and without pre-irradiation annealing), the effect of the thermally induced size changes on NPs was evaluated and concluded as small.

Table 1. Thermal history of each sample. O: applied, X: not applied.

Pre-Irradiation Annealing at 591 K for 5 h	Irradiation Temperature (K)	Ion Irradiation at Specified Temperature (120 MeV Ag ⁹⁺ Ions to 1.0×10^{14} ions/cm ²)
X	300	O
X		X
O		O
O		X
X	433	O
X		X
O		O
X	515	O
X		X
O		O
X	591	O
X		X
O		O

A standard ultraviolet- and visible-range (UV-vis) dual-beam spectrophotometer was used for the OLD spectroscopy measurements in the wavelength region of 215–800 nm with a resolution of 1 nm; a pair of optical polarizers (extinction ratio $< 5 \times 10^{-5}$ each) were used. All the OLD spectroscopy measurements were carried out at RT. A sample was set between two polarizers, P and A, and illuminated by linearly polarized monochromatic light from the spectrophotometer through the first polarizer P. Light transmitted through the sample was detected through the second polarizer A, whose polarization angle was set to the same as the polarizer P. The second polarizer A removes the birefringence signal [18] from the OLD signal, while the former is much weaker than the latter. The detected transmittance was shown in the form of optical density ($OD = -\log_{10} T$) without reflection correction, where T denotes the transmittance. To represent a value of the elongation degree from a pair of polarized spectra at each IT, the elongation η was defined as,

$$\eta(T_{\text{irrad}}) = \int_{340 \text{ nm}}^{800 \text{ nm}} OD(\lambda, 0^\circ, T_{\text{irrad}}) - OD(\lambda, 90^\circ, T_{\text{irrad}}) d\lambda. \quad (1)$$

The elongation η was determined with the spectra measured at the polarization angle of 0 and 90°. When the polarization plane includes the major axes of NPs, the polarization angle is defined as 0°. Since the point-defect-related absorption was detected at the wavelength region shorter than 340 nm, the shorter bound of the integral interval was set to 340 nm.

Some samples were thinned down to a thickness of less than 100 nm by using 30 keV Ga⁺ focused ion beam (FIB) milling. TEM observation was conducted using JEOL JEM-2100 transmission electron microscopes (JEOL, Tokyo, Japan) with an operating voltage of 200 kV.

3. Results

3.1. XTEM Observation

Figure 1a exhibits cross-sectional TEM (XTEM) images of a silica sample implanted with 60 keV V⁺ ions to a fluence of 1.0×10^{17} ions/cm², i.e., as-implanted sample. Nearly spherical NPs were observed with a certain size distribution. Since the NPs overlap with each other in the image, the determination of the size distribution was not easy.

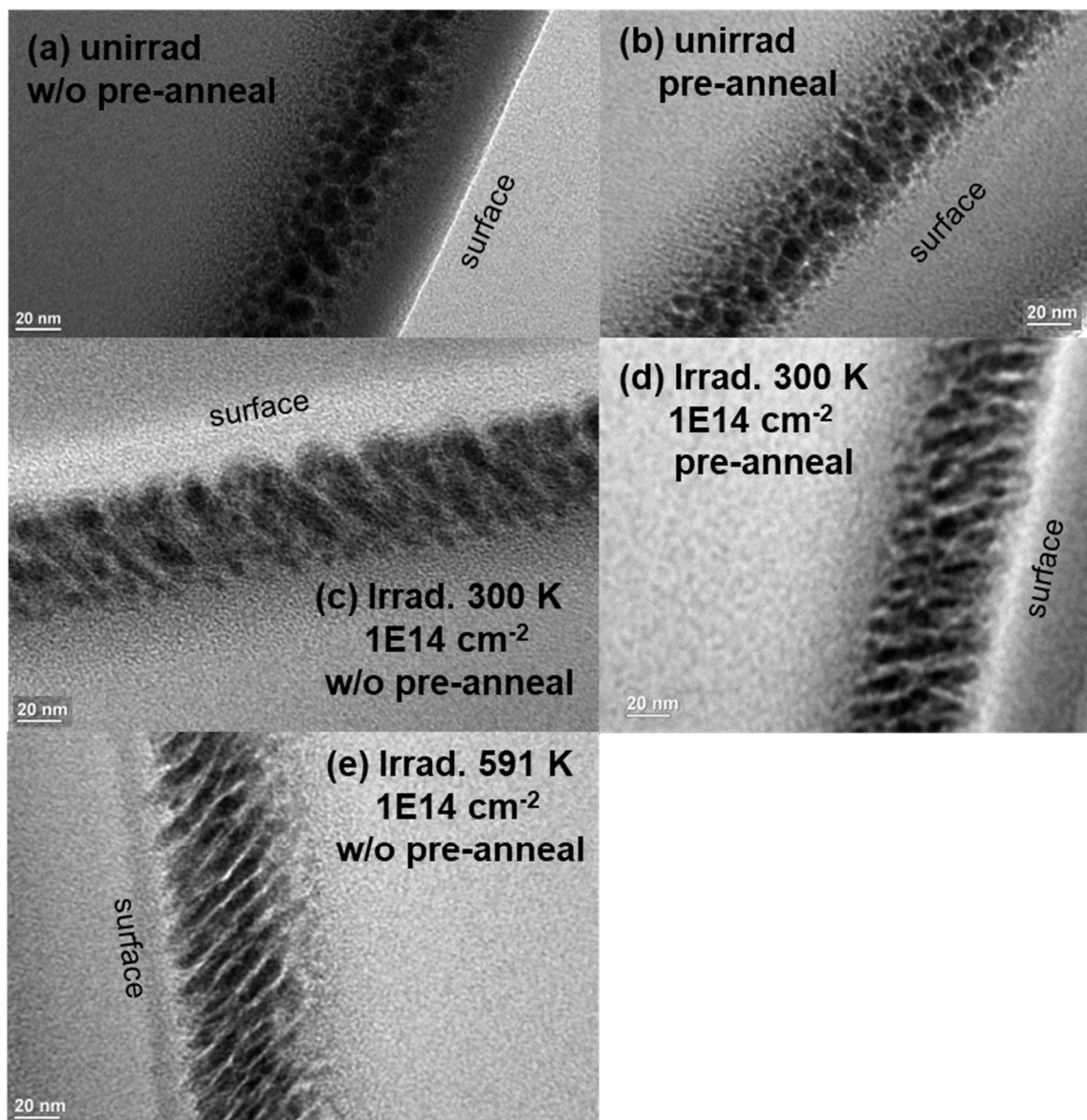


Figure 1. Cross-sectional transmission electron microscopy (XTEM) images of vanadium nanoparticles (NPs) embedded in SiO_2 : (a) as-implanted state without annealing, (b) annealed in a vacuum at 591 K for 5 h. (c,d) irradiated at 300 K with 120 MeV Ag^{9+} ion to a fluence of 1.0×10^{14} ions/ cm^2 , (c) without and (d) with the pre-irradiation annealing in a vacuum at 591 K for 5 h. (e) irradiated at 591 K with 120 MeV Ag^{9+} ions without the pre-irradiation annealing.

Since the IT dependence is the target of this paper, the thermally induced size change of the NPs is a critical issue, particularly when the elongation is induced at high ITs. To estimate the degree of the size changes, another set of as-implanted samples was annealed in a vacuum using the high-temperature irradiation chamber at the highest IT of 591 K for the typical irradiation duration of 5 h. The corresponding XTEM image is shown in Figure 1b. Since vanadium has high thermal stability and the annealing temperature of 591 K is not so high, the size distribution of the annealed sample looks like that of the sample without annealing. Therefore, the thermal-induced size changes of NPs in the present experiments are small.

To further confirm the thermally induced effects on the elongation of V NPs, a pair of V-implanted samples with/without the annealing at 591 K for 5 h were irradiated with 120 MeV Ag^{9+} ions at RT under the same conditions. XTEM images of the samples are

shown in Figure 1c,d without and with the pre-annealing, respectively. Comparing the unirradiated samples (Figure 1a,b) with the irradiated samples (Figure 1c,d), the overwhelming elongation starting from the unirradiated spherical NPs is clear. As later shown in Section 3.2, the degree of the elongation determined by OLD spectroscopy was comparable between the samples with/without the pre-irradiation annealing. This conclusion is supported by the TEM images of Figure 1c,d.

As shown in Figure 1e, the sample irradiated at 591 K exhibits nearly comparable but slightly clearer elongation than the samples irradiated at 300 K. This observation is counterevidence to the IH effect, since the deformation yield A of the IH effect in silica at 590 K decreases to 37% of that at 300 K [9]. However, the elongation at 591 K is comparable to or slightly higher than that at 300 K as shown in Figure 1c,e. A slightly higher degree of elongation in the sample irradiated at 591 K is confirmed by OLD spectroscopy, as shown in Section 3.2.

3.2. Optical Linear Dichroism (OLD) Spectroscopy

Figure 2 exhibits optical density spectra of V NPs embedded in silica, all of which were measured at RT, while the irradiations with 120 MeV Ag^{9+} ions had been carried out at a specified temperature between 300 and 591 K. A pair of samples was prepared for each IT: Both the samples were mounted in the high-temperature irradiation chamber and were maintained at the specified temperature. Only one of the two samples was irradiated with 120 MeV Ag^{9+} ions to the fixed fluence of 1.0×10^{14} ions/cm². The other sample was not irradiated but maintained at the same temperature during the ion irradiation periods of ~5 h. After cooling, with the sample temperature down to nearly RT, the pair of samples was extracted from the chamber. Then the optical density spectra were collected later using linearly polarized light with the polarization angle of 0 and 90°.

The spectra collected at the polarization angle of 0 and 90° are indicated by solid curves and broken curves in Figure 2, respectively. With maintaining the samples at any temperatures between 300 and 591 K without irradiations, almost no deviation was observed between the 0°- and the 90°-polarizations. While these observations are quite reasonable, they are necessary to avoid criticism.

After the ion irradiations, the 0°-spectra and 90°-spectra increase and decrease, respectively, and the basements of the curves almost maintain the shapes of the curves. These are typical changes in the OLD spectra against the elongation of V NPs [15].

It should be noted that a strong peak appeared around 5 eV after 120 MeV Ag^{9+} ion irradiation as shown in Figure 2. However, this peak is ascribed to point defects of silica, which are called oxygen-deficient centers of type II (ODC-II) [19]. This peak is observed in SiO_2 irradiated with SHIs [20] and even irradiated with low energy ions of 60 keV B dimmer ions [21]. It is reported that ODC-II absorption steeply decreases with raising the temperature to 200 °C (473 K) [22]. According to our unpublished data of isochronal vacuum annealing of silica irradiated with 200 MeV Xe ions, the absorption intensity of the ODC-II does not decrease even after annealing at 373 K for 10 min. However, the isochronal annealing for 10 min each at 473, 573, and 673 K, the absorption intensity decreased to 60, 25, and less than 5% of the value without annealing, respectively. Since the ODC-II defects may be formed during the irradiation period, a direct comparison is difficult between the isochronal annealing and the irradiation at high temperature. A decrease in the ODC-II absorption confirms that the IT certainly increases.

To express the degree of the shape elongation of NPs by a single numerical value, the quantity “elongation η ” defined by Equation (1) was plotted in Figure 3 for each IT. As described in Section 2, two sets of samples were prepared: While one set of samples was irradiated with the SHIs at specified Its after pre-irradiation annealing at 591 K for 5 h, the other set of samples was irradiated with the same conditions without the pre-irradiation annealing.

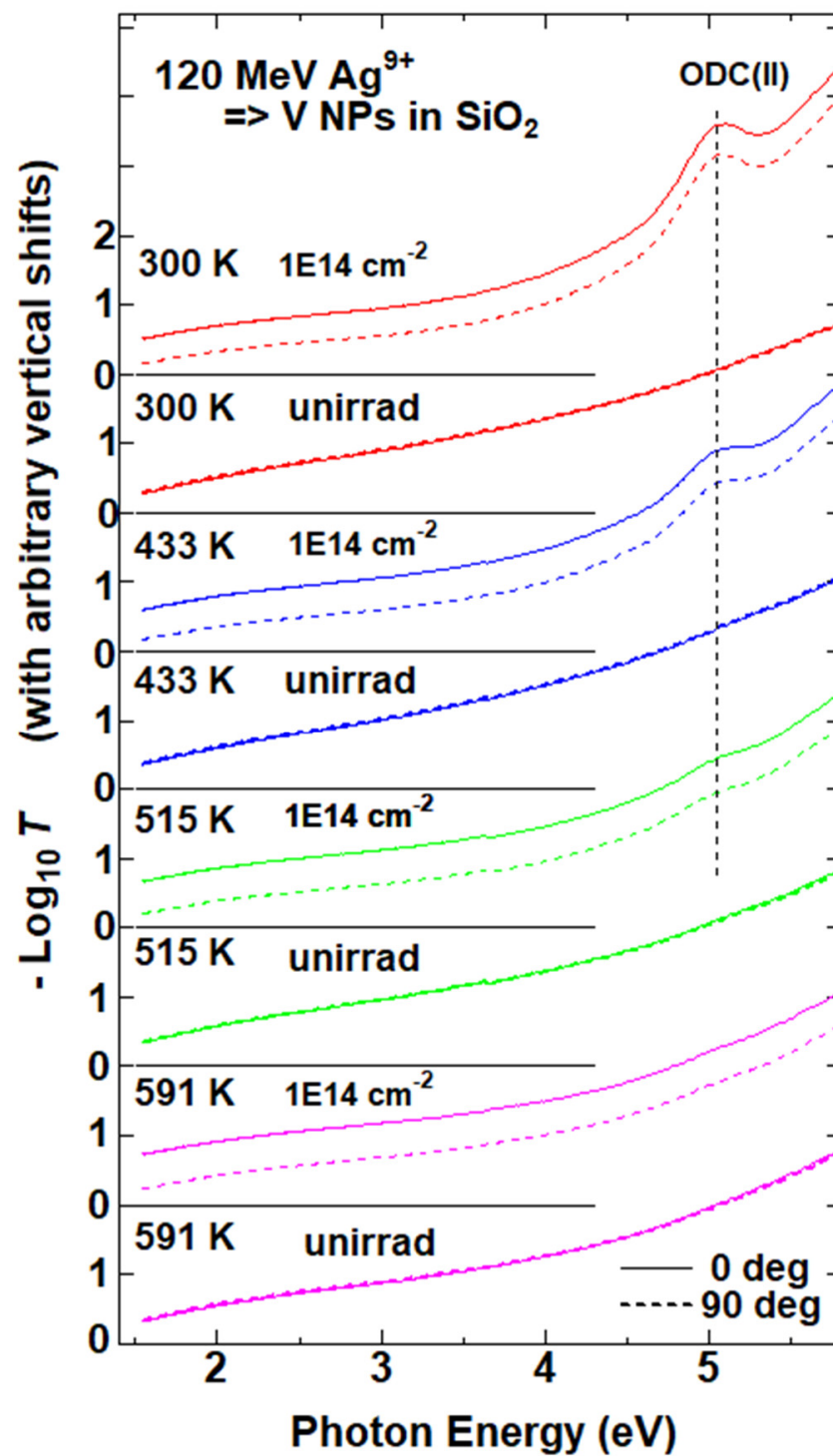


Figure 2. Optical density spectra of V NPs in silica, unirradiated and irradiated with 120 MeV Ag⁹⁺ ions to the fixed fluence of 1.0×10^{14} ions/cm² at the temperatures indicated in the figure. Unirradiated samples were not irradiated but maintained at the indicated temperatures for a duration of 5 h. All the spectra were measured at room temperature after cooling down from the irradiated temperatures. The solid (broken) curves indicate the spectra measured with linearly polarized light at a polarization angle of 0° (90°). The 0° polarization plan includes the major axes of the NPs, if elongated, while the 90° polarization plane is perpendicular to it. The spectra with different irradiation temperatures or fluences are vertically shifted with each other for clarity. Horizontal lines indicate the offsets of each spectrum. A peak at ~5 eV is ascribed to the ODC(II) point defects of silica [19].

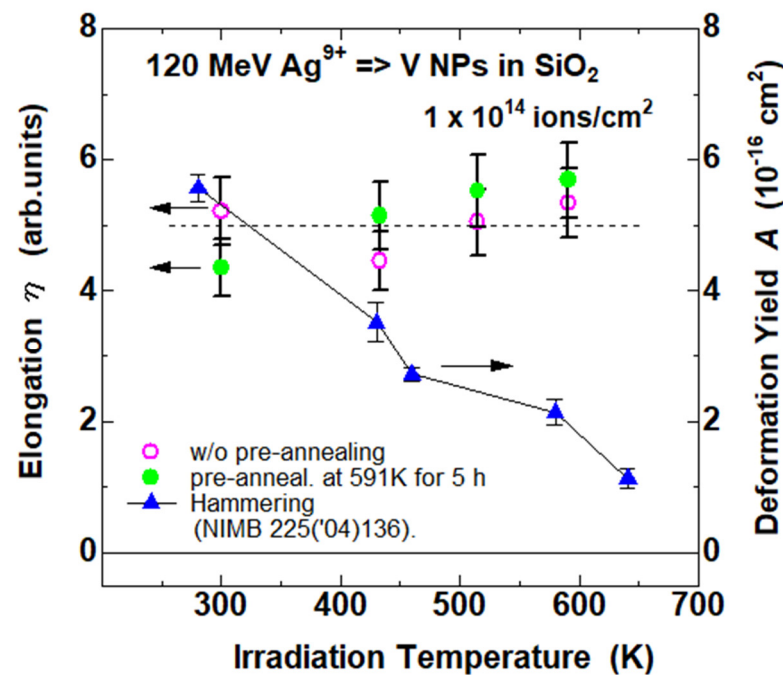


Figure 3. Irradiation temperature dependence of the degree of the shape elongation of V NPs in SiO₂, defined by Equation (1), induced by irradiation with 120 MeV Ag⁹⁺ ions to a fluence of 1.0×10^{14} ions/cm², without pre-annealing (open circles) and with pre-annealing of 591 K for 5 h (closed circles). The dependence of the deformation yield A of SiO₂ ascribed to the ion hammering effect was collected from Ref. [9]. Solid lines and horizontal broken lines are guides for eyes.

The data points of the elongation η with/without the pre-annealing were plotted with open and closed circles, respectively. The errors of the elongation were set as $\pm 10\%$ of the elongation value. The main source of the errors comes from the fluctuation of the ion fluence via that of the beam current since the irradiation duration is very long at nearly 5 h. The data with and without the pre-irradiation annealing at the same Its were the same within the experimental errors. The averaged values were almost constant or slightly increased with rising the IT from 300 to 591 K. This behavior is consistent with the results of TEM observation shown in Figure 1, as the elongation of NPs looks clearer in the sample irradiated at 591 K than those irradiated at 300 K.

It is known that the deformation of silica by the IH effect becomes less prominent at higher IT [9]. The IT dependence of the deformation yield A of the IH effect in silica irradiated with 340 MeV Xe ions was collected from Ref. [9] and plotted in Figure 3 by triangles. The comparisons of the IT dependences of the elongation of NPs and the deformation of silica by the IH effect indicate that the former slightly increases but the latter steeply decreases with increasing the IT, indicating that the IH effect is not the main mechanism of the shape elongation of NPs.

4. Discussion

We have pointed out three observations which are inconsistent with the IH effect as the origin of the elongation of NPs: (i) and (ii) were reported in past literature [8,10,11] and (iii) is in this work.

(i) It is confirmed that the shape elongation of NPs is induced even at the first collision of the ion to each NP [8], but the single ion impact is not expected to induce NP elongation according to the synergy model with the IH effect and NP melting by i-TS effect. Since this observation required the detection of small elongation at low fluences, the detection was attained using OLD spectroscopy [8,23]. Furthermore, silica shows compaction with the first ion impact and the IH effect is only induced after almost all the surface is covered by ion impacts. Therefore, it has again been supported that the elongation induced with

the first ion impacts cannot be explained by the IH effect [10]. Since the NPs in silica are formed by low energy (60 keV) ion implantation, we might be criticized that the IH effect could be induced from the beginning of the SHI irradiation, because the full of compaction would be built up by the 60 keV metal ion implantation. To answer this criticism, some of the samples prepared by Ion implantation were annealed at 600 °C (873 K) to recover them from the compacted state and then irradiated them with SHIs. Similar fluence dependence was observed, indicating that NP elongation does not depend on the existence of the compaction or the IH effect.

(ii) Coincidence of the ion incident angle and the NP elongation angle. See [11].

(iii) The different irradiation temperature dependencies between the IH effect and the NP elongation. It should be noted that the degree of elongation was determined by OLD spectroscopy.

When we reported observation (i), one of the criticisms was whether the OLD signal really came from the elongation of NPs or not. This criticism could be applied to the present case of IT dependence since it was detected by OLD spectroscopy. The single ion impact could form certain kinds of anisotropic point defects in SiO₂, which possess optical linear dichroism. The observed OLD signal could not be from the elongated NPs but from the anisotropic point defects. However, this possibility was easily excluded: The OLD spectra have material-dependent spectral shapes, i.e., the OLD spectra of Zn NPs have completely different shapes from those of V NPs. Furthermore, the OLD spectra are approximately calculated from the Rayleigh theory of optical extinction spectra of ellipsoids [24]. The calculated OLD spectra for elongated metal NPs matched well with the experimentally observed ones. These facts strongly support that the observed OLD signal is ascribed to elongated metal NPs, not from anisotropic point defects in silica. In addition, the TEM results also show the elongation of NPs in the present cases.

5. Conclusions

Irradiation temperature dependence of the shape elongation efficiency of V NPs in SiO₂ was evaluated between 300 and 591 K. The V NPs were formed in SiO₂ by V ion implantation of 60 keV to the fluence of 1.0×10^{17} ions/cm². Vanadium was selected because of its highest m.p. of 1910 °C (2183 K) among all the metal NPs which exhibit shape elongation. Because of the high m.p., thermal changes in sizes in metal NPs are negligible compared with other low m.p. metal NPs. The evaluation of the NP elongation was carried out by TEM observation and OLD spectroscopy. Since the V NPs were formed by low energy ion implantation of 60 keV, the interparticle distances were so short that the disassembly of the overlapped images to each NP was quite difficult. However, TEM images showed that the elongation in the sample irradiated at 591 K was slightly more pronounced than that irradiated at 300 K. This observation was qualitatively inconsistent with the previous literature on the IH effect of silica, which reported the reduction of the deformation yield *A* of ~37% with increasing the temperature from 300 to 590 K.

The quantitative evaluation was carried out using OLD spectroscopy. According to the OLD signal, the elongation degree of V NPs was almost constant or slightly increases with increasing the irradiation temperature from 300 to 591 K. The deformation yield *A* of the IH effect in SiO₂ steeply decreases with increasing the IT. Consequently, the IT dependence of the NP elongation and that of the IH effect are qualitatively different. Therefore, the IH effect cannot be considered as the origin of the NP elongation.

Author Contributions: Basic conceptualization, H.A.; realistic implementation plan, H.A., S.A.K., P.K.K. and D.K.; sample preparation, H.A.; temperature calibration, S.A.K., P.K.K. and D.K.; ion irradiation, S.A.K., P.K.K. and D.K.; Characterization, H.A. All authors have read and agreed to the published version of the manuscript.

Funding: This research was funded by JSPS-KAKENHI, Grant number 22K04990.

Institutional Review Board Statement: Not applicable.

Informed Consent Statement: Not applicable.

Data Availability Statement: The datasets and materials generated during the current study are available from the corresponding author on reasonable request.

Acknowledgments: SHI irradiations were carried out in IUAC, New Delhi via BTR No 57401 and 60401. The authors are grateful to the staff of the accelerator facilities at IUAC. TEM observation was performed using the facility of the NIMS TEM station. The authors also acknowledge the Indo-Japan personal exchange program for supporting the research under project No. DST/INT/JSPS/P-111/2011.

Conflicts of Interest: The authors declare no conflict of interest.

References

1. D'Orleans, C.; Stoquert, J.P.; Estournès, C.; Cerruti, C.; Grob, J.J.; Guille, J.L.; Haas, F.; Muller, D.; Richard-Plouet, M. Anisotropy of Co nanoparticles induced by swift heavy ions. *Phys. Rev. B* **2003**, *67*, 220101. [CrossRef]
2. Roorda, S.; van Dillen, T.; Polman, A.; Graf, C.; van Blaaderen, A.; Kooi, B.J. Aligned gold nanorods in silica made by ion irradiation of core-shell colloidal particles. *Adv. Mater.* **2004**, *16*, 235–237. [CrossRef]
3. Snoeks, E.; van Blaaderen, A.; van Dillen, T.; van Kats, C.M.; Brongersma, M.L.; Polman, A. Colloidal Ellipsoids with Continuously Variable Shape. *Adv. Mater.* **2000**, *12*, 1511–1514. [CrossRef]
4. Klaumunzer, S. Modification of nanostructures by high-energy ion beams. *Nucl. Instrum. Methods Phys. Res. B* **2006**, *244*, 1–7. [CrossRef]
5. Harkati Kerboua, C.; Lamarre, J.M.; Chicoine, M.; Martinu, L.; Roorda, S. Elongation of gold nanoparticles by swift heavy ion irradiation: Surface plasmon resonance shift dependence on the electronic stopping power. *Thin Solid Film.* **2013**, *527*, 186–192. [CrossRef]
6. Dufour, C.; Toulemonde, M. Models for the description of track formation. In *Ion Beam Modification of Solids*; Wesch, W., Wendler, E., Eds.; Springer Series in Surface Sciences; Springer International Publishing: Cham, Switzerland, 2016; Volume 61, pp. 63–104. [CrossRef]
7. Leino, A.A.; Pakarinen, O.H.; Djurabekova, F.; Nordlund, K.; Kluth, P.; Ridgway, M.C. Swift Heavy Ion Shape Transformation of Au Nanocrystals Mediated by Molten Material Flow and Recrystallization. *Mater. Res. Lett.* **2014**, *2*, 37–42. [CrossRef]
8. Amekura, H.; Ishikawa, N.; Okubo, N.; Ridgway, M.C.; Giulian, R.; Mitsuishi, K.; Nakayama, Y.; Buchal, C.; Mantl, S.; Kishimoto, N. Zn nanoparticles irradiated with swift heavy ions at low fluences: Optically-detected shape elongation induced by nonoverlapping ion tracks. *Phys. Rev. B* **2011**, *83*, 205401. [CrossRef]
9. Klaumunzer, S. Ion tracks in quartz and vitreous silica. *Nucl. Instrum. Methods Phys. Res. B* **2004**, *225*, 136–153. [CrossRef]
10. Amekura, H.; Okubo, N.; Tsuya, D.; Ishikawa, N. Counterevidence to the ion hammering scenario as a driving force for the shape elongation of embedded nanoparticles. *AIP Adv.* **2017**, *7*, 085304. [CrossRef]
11. Amekura, H.; Kluth, P.; Mota-Santiago, P.; Sahlberg, I.; Jantunen, V.; Leino, A.A.; Vazquez, H.; Nordlund, K.; Djurabekova, F. On the mechanism of the shape elongation of embedded nanoparticles. *Nucl. Instrum. Methods Phys. Res. Sect. B Beam Interact. Mater. At.* **2020**, *475*, 44–48. [CrossRef]
12. Slablab, A.; Isotalo, T.J.; Mäkitalo, J.; Turquet, L.; Coulon, P.-E.; Niemi, T.; Ulysse, C.; Kociak, M.; Mailly, D.; Rizza, G.; et al. Fabrication of Ion-Shaped Anisotropic Nanoparticles and their Orientational Imaging by Second-Harmonic Generation Microscopy. *Sci. Rep.* **2016**, *6*, 37469. [CrossRef] [PubMed]
13. Royal Society of Chemistry, Periodic Table. Available online: <https://www.rsc.org/periodic-table/element/23/vanadium> (accessed on 20 March 2023).
14. Amekura, H.; Sele, M.L.; Ishikawa, N.; Okubo, N. Thermal stability of embedded metal nanoparticles elongated by swift heavy ion irradiation: Zn nanoparticles in a molten state but preserving elongated shapes. *Nanotechnology* **2012**, *23*, 095704. [CrossRef] [PubMed]
15. Amekura, H.; Ishikawa, N.; Okubo, N.; Nakayama, Y.; Mitsuishi, K. Asynchronous melting of embedded metal nanoparticles and silica matrix for shape elongation induced by swift heavy ion irradiation. *Nucl. Instrum. Methods Phys. Res. Sect. B Beam Interact. Mater. At.* **2011**, *269*, 2730–2733. [CrossRef]
16. Kulriya, P.K.; Kumari, R.; Kumar, R.; Grover, V.; Shukla, R.; Tyagi, A.K.; Avasthi, D.K. In-situ high temperature irradiation setup for temperature dependent structural studies of materials under swift heavy ion irradiation. *Nucl. Instrum. Methods Phys. Res. Sect. B Beam Interact. Mater. At.* **2015**, *342*, 98–103. [CrossRef]
17. Rizza, G.; Coulon, P.E.; Khomenkov, V.; Dufour, C.; Monnet, I.; Toulemonde, M.; Perruchas, S.; Gacoin, T.; Mailly, D.; Lafosse, X.; et al. Rational description of the ion-beam shaping mechanism. *Phys. Rev. B* **2012**, *86*, 035450. [CrossRef]
18. Amekura, H.; Okubo, N.; Ishikawa, N. Optical birefringence of Zn nanoparticles embedded in silica induced by swift heavy-ion irradiation. *Opt. Express* **2014**, *22*, 29888–29898. [CrossRef]
19. Skuja, L. Optically active oxygen-deficiency-related centers in amorphous silicon dioxide. *J. Non-Cryst. Solids* **1998**, *239*, 16–48. [CrossRef]

20. Amekura, H.; Okubo, N.; Ren, F.; Ishikawa, N. Swift heavy ion irradiation to ZnO nanoparticles: Steep degradation at low fluences and stable tolerance at high fluences. *J. Appl. Phys.* **2018**, *124*, 145901. [[CrossRef](#)]
21. Amekura, H.; Kishimoto, N. Effects of high-fluence ion implantation on colorless diamond self-standing films. *J. Appl. Phys.* **2008**, *104*, 063509. [[CrossRef](#)]
22. Griscom, D.L. Optical properties and structure of defects in silica glass. *J. Ceram. Soc. Jpn.* **1991**, *99*, 923–942. [[CrossRef](#)]
23. Amekura, H.; Mohapatra, S.; Singh, U.B.; Khan, S.A.; Kulriya, P.K.; Ishikawa, N.; Okubo, N.; Avasthi, D.K. Shape elongation of Zn nanoparticles in silica irradiated with swift heavy ions of different species and energies: Scaling law and some insights on the elongation mechanism. *Nanotechnology* **2014**, *25*, 435301. [[CrossRef](#)] [[PubMed](#)]
24. Bohren, C.F.; Huffman, B.R. *Absorption and Scattering of Light by Small Particles*; John Wiley & Sons, Inc.: New York, NY, USA, 1983.

Disclaimer/Publisher's Note: The statements, opinions and data contained in all publications are solely those of the individual author(s) and contributor(s) and not of MDPI and/or the editor(s). MDPI and/or the editor(s) disclaim responsibility for any injury to people or property resulting from any ideas, methods, instructions or products referred to in the content.